

Flow and correlation phenomena measurements in pp, pPb and PbPb collisions at CMS

Sandra S. Padula (on behalf of the CMS Collaboration)^{1,*}

¹Universidade Estadual Paulista (UNESP), São Paulo, SP, Brazil

Abstract. The quark-gluon plasma created in high energy collisions of large nuclei exhibits strong anisotropic collective behavior as a nearly perfect fluid, flowing with little frictional resistance or viscosity. It has been investigated extensively over the past years employing two or more particle correlations. An overview of collective flow and particle correlation measurements at CMS as a function of transverse momentum, pseudorapidity, event multiplicity, for both charged hadrons or identified particles will be presented. These results are compared among pp, pPb and PbPb systems and several aspects of their intriguing similarities are discussed.

1 Introduction

The state of deconfined quarks and gluons predicted by quantum chromodynamics, the quark-gluon plasma (QGP), was discovered at the Relativistic Heavy Ion Collider (RHIC) and found to be a strongly coupled medium, behaving as a nearly perfect fluid [1]. This finding was possible through the observation of anisotropic azimuthal correlations that can be associated to the collective properties of the hot and dense medium formed in such high energy collisions. Another important property observed at RHIC was the quench of the jets traversing the hot and dense medium, an effect which was more pronounced as the overlapping of the interacting nuclei increased from peripheral to head-on relativistic heavy ion collisions. At the Large Hadron Collider (LHC), the QGP has been further extensively investigated through a myriad of measurements performed over the recent years. In particular, the extension of the measurement of azimuthal correlations to particles with very high transverse momentum p_T , has added significant new insights into these observations, connecting both effects: in the low p_T region, the anisotropic azimuthal correlations are associated with the hydrodynamic collective flow, whereas in very high p_T realm, such correlations may reflect the path lengths followed by the quenched jet, reflecting the in-medium parton energy loss.

An additional remarkable discovery in AA collisions at RHIC energies was the “ridge-like” two-hadrons correlations, where particles very close in the azimuthal direction ($\Delta\phi \sim 0$) are correlated over a wide region in their relative pseudorapidity (up to $\Delta\eta \sim 4$). Amazingly, similar correlations were discovered in 2010 at the LHC in high multiplicity events produced in pp collisions at 7 TeV [2] and, some time later, also in pPb collisions, raising questions about the possible common nature of the systems formed in pp, pA and AA collisions.

*e-mail: sandra.padula@cern.ch

Results related to the phenomena described above are reported in this paper. First, azimuthal correlations in $PbPb$ collisions at $\sqrt{s_{NN}} = 5.02$ are presented, extending from low transverse momentum ($1 < p_T < 3$ GeV/c), up to very large p_T (≈ 100 GeV/c) [3]. The measurements of the corresponding Fourier coefficients are performed employing the scalar product method, by correlating charged tracks with the energy deposited in the hadronic forward calorimeters, as well as the multi-particle cumulant.

Next, measurements of two- and multi-particle angular correlations are discussed for high multiplicity events in pp collisions at $\sqrt{s} = 13$ TeV. Such correlations are investigated with unidentified charged particles (h^\pm), as well as reconstructed K_S^0 and Λ particles [4]. The results of v_2 and v_3 harmonics extracted from two-particle correlations are studied as functions of particle p_T and event multiplicity. The residual contribution of back-to-back jet correlations to the ridge phenomenon is estimated and removed by subtracting correlations obtained from very low multiplicity pp events. For high-multiplicity pp events, a mass ordering is observed for the v_2 values of charged hadrons (mostly pions), K_S^0 , and $\Lambda/\bar{\Lambda}$, with lighter particle species exhibiting a stronger azimuthal anisotropy signal below $p_T \approx 2$ GeV/c. The v_2 signals are also extracted from four- and six-particle correlations using the cumulant method, on the search for a possible collective nature of the correlations. The pp results are directly compared to those found for pPb at 5 TeV and PbPb at 2.76 TeV collisions over a broad range of similar multiplicities, revealing similar observations in the three systems. These findings suggest a collective origin for the observed long-range correlations in high-multiplicity pp collisions.

Finally, a recent development is discussed, which allows for more deeply scrutinizing the final-state azimuthal anisotropy in different colliding systems by measuring the correlations between Fourier harmonic coefficients. In nucleus-nucleus collisions, these correlations have been shown to be strongly sensitive to initial-state fluctuations and to medium transport coefficients [5]. In what follows, the measurement of anisotropy harmonics (v_n , $n = 2 - 4$) and event-by-event correlations of different v_n , using data collected by the CMS experiment are presented for pp at 13 TeV, pPb at 5.02 and 8 TeV, and PbPb collisions at 5.02 TeV [6]. The v_n results are extracted via long-range ($\Delta\eta > 2$) two-particle correlations as a function of event multiplicity. Event-by-event correlations of v_2 versus v_3 and v_2 versus v_4 are measured using the four-particle Symmetric Cumulant (SC) method for these three colliding systems.

2 The CMS experiment

The CMS detector has nearly 4π solid angle acceptance and an extended coverage of more than ten units in pseudorapidity ($\eta = -\log[\tan(\theta/2)]$, with θ being the polar angle along the beam direction). Its large superconducting solenoid of 6 m internal diameter, with 3.8 T axial magnetic field, is surrounding the three-layer silicon pixel and the strip tracker, the crystal electromagnetic calorimeter, and a brass/scintillator hadron calorimeter. Muons are measured in gas-ionization detectors embedded in the steel return yoke. In addition to these detectors, CMS has extensive forward calorimetry, in particular two steel/quartz-fiber Cerenkov forward hadronic calorimeters (HF, $2.9 < |\eta| < 5.2$). A complete description of the CMS detector can be found in Ref.[7].

3 Anisotropy harmonics measured up to very high p_T

In non-central collisions, the eccentricities in the overlapping region of the two colliding nuclei result in spatial asymmetries. After the local thermal equilibrium is attained following the strong rescattering of the partons in the initial state, such asymmetries drive a collective anisotropic expansion, which is faster along the short axis of the almond shaped initial overlapping region due to the largest pressure gradient, resulting in the observed azimuthal anisotropies. The azimuthal dependence of the

particle yield can be written in terms of an harmonic expansion, in which the Fourier coefficients v_2 and v_3 correspond to the elliptic and triangular flow, respectively. For characterizing the anisotropy of the azimuthal distribution of charged particles produced in PbPb collisions at $\sqrt{s_{NN}} = 5.02$ TeV these coefficients are measured with data collected by the CMS experiment. The scalar product method is employed for measuring the $v_2\{\text{SP}\}$ and $v_3\{\text{SP}\}$ anisotropy coefficients as a function of p_T up to 100 GeV/c, for several collision centrality intervals in the overall range 0-60%. The details about data samples, experimental procedures, the scalar product method and the systematic uncertainties, can be found in Ref. [3]. The results are shown in Fig. 1 left panel, with statistical and systematic uncertainties represented by bars and shaded boxes, respectively. In Fig. 1 left panel, the v_2 and v_3 results are compared to the CUJET3.0 [9] and SHEE [8] models for several centrality bins. An essential difference between these two models is that in SHEE is that it includes initial-state geometry fluctuations (in addition to linear path-length dependence of parton energy loss), whereas CUJET3.0 uses a smooth hydrodynamic background (and uses perturbative quantum chromodynamics (pQCD) calculations to describe the hard parton interactions). Calculations from SHEE show a good agreement with the data, over the wide p_T and centrality ranges probed in this analysis.

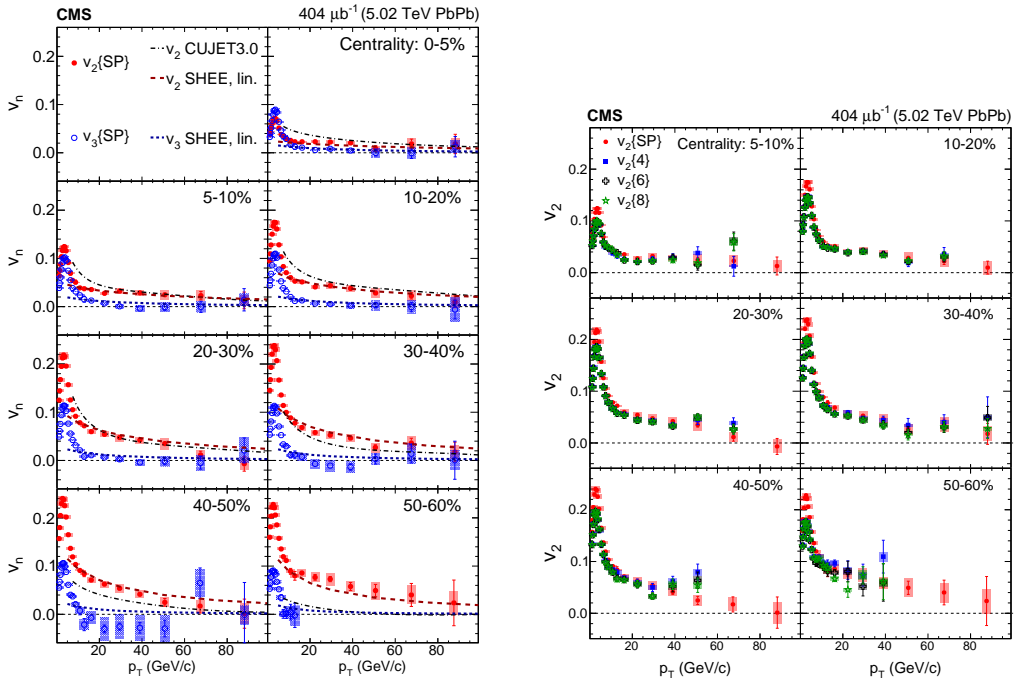


Figure 1. Left panel: Results of $v_2\{\text{SP}\}$ and $v_3\{\text{SP}\}$ measured in PbPb collisions at $\sqrt{s_{NN}} = 5.02$ TeV are shown in several centrality windows as a function of the transverse momentum p_T . Right panel: Results of $v_2\{\text{SP}\}$ and multi-particle cumulants $v_2\{4\}$, $v_2\{6\}$, $v_2\{8\}$ are shown as a function of p_T in six centrality ranges in the same collisions. Statistical and systematic uncertainties are represented, respectively, by bars and shaded boxes. The plots are from Ref. [3].

It can be seen that, for all centralities, $v_2\{\text{SP}\}$ shows a rapid rise up to $p_T \approx 3$ GeV/c and then falls fast up to $p_T \approx 10$ GeV/c, decreasing more slowly for higher values of the transverse momentum,

and remaining non-zero up to very high p_T . At low- p_T , $v_2\{\text{SP}\}$ increases from most central to mid-peripheral events (30-40%), and then decreases toward more peripheral ones, showing a similar p_T behavior in all measured centralities. The $v_3\{\text{SP}\}$ values are also shown in Fig. 1 left panel, exhibiting a similar behavior as that of $v_2\{\text{SP}\}$ for the same centrality ranges, although being practically centrality independent for low p_T . Besides, the measured $v_3\{\text{SP}\}$ shows non-zero values up to $p_T \approx 20$ GeV/c, which is consistent with picturing the system as being subjected to fluctuating initial conditions (the odd harmonics would be identically zero, by symmetry, if the initial conditions were described by nucleons distributed in a uniform and rotationally invariant way in both nuclei).

In order to investigate the origin of the non-zero anisotropy coefficients up to such high p_T and to explore its possible collective nature, the v_2 values are also measured by correlating 4, 6 and 8 particles. The Q -cumulant method [11] is used to measure $v_2\{4\}$, $v_2\{6\}$, $v_2\{8\}$, providing a fast, exact (free of approximations), and unbiased (no interference between different harmonics) evaluation of the cumulants. The method is also subjected to non-flow effects since, if M particles are produced in a collisions, direct k -particle correlations are of order $1/M^{k-1}$, so that they become smaller as k increases. Therefore, the 4^{th} -, 6^{th} -, 8^{th} -order cumulant results are expected to be much less affected by non-flow contributions than the second-order one. The cumulants are expressed in terms of the moments of the magnitude of the corresponding flow vectors Q_n . The details of the technique and measurement are in Ref. [3]. The corresponding results are shown in Fig. 1 right panel, from which it can be seen that, in the range $p_T < 3$ GeV/c, $v_2\{\text{SP}\} > v_2\{4\} \approx v_2\{6\} \approx v_2\{8\}$, a result which is consistent with the expectations from hydrodynamics. For $p_T > 10$ GeV/c, $v_2\{\text{SP}\} \approx v_2\{m\}$, providing strong evidence that collective anisotropic particle emission in heavy ion collisions extends to very high p_T . Although the nature of the collectivity at high p_T may be related to the jet quenching phenomena, these observations of anisotropies at both low and high p_T are likely related to the initial state anisotropies and event-by-event fluctuations, posing a challenge to be jointly described by theoretical models.

4 Signs of collectivity also seen in pp and pPb collisions

The long-range two-particle correlation phenomena in high-multiplicity in small systems had its investigation further extended by measuring of two- and multi-particle azimuthal correlations with unidentified charged particles, as well as correlations of reconstructed V^0 particles (i.e., K_S^0 and $\Lambda/\bar{\Lambda}$) in pp collision at $\sqrt{s_{NN}} = 5, 7$ and 13 TeV energies [4]. The technique used for investigating two-hadrons correlations defines, for each track multiplicity class, “trigger” particles as charged particles or V^0 candidates with $|\eta| < 2.4$, originating from the primary vertex within a given p_T^{trig} range. Particle pairs are then formed by associating each trigger particle with the remaining charged primary tracks with $|\eta| < 2.4$ and from a specified p_T^{assoc} interval (which can be either the same as or different from the p_T^{trig}). A pair is removed if the associated particle is the daughter of any trigger V^0 candidate (this contribution is negligible since associated particles are mostly primary tracks). The background to such signal combination is constructed by pairing the trigger particles in each event with the associated charged particles from 20 different randomly selected events in the same 0.5 cm wide longitudinal vertex position (z_{vtx}) range and from the same track multiplicity class. The same-event and mixed-event pair distributions are first calculated for each event, and then averaged over all the events within the track multiplicity class. Details of this analysis, containing the data samples, event selections, as well as a complete description of the technique used for studying dihadron correlations, and the estimate of corresponding systematic uncertainties can be found in Ref. [4] and in references therein.

The v_2 harmonics extracted from two-particle correlations are studied as functions of particle p_T and event multiplicity and are shown in Fig. 2. The left plot shows the measurements in the low

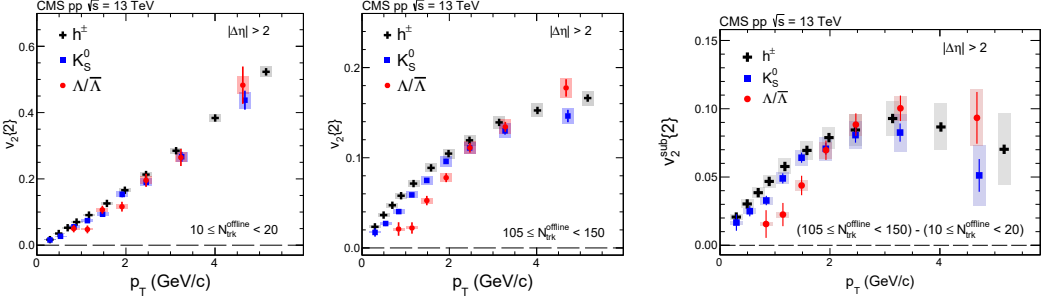


Figure 2. Results of $v_2\{2\}$ for inclusive charged particles, K_S^0 and $\Lambda/\bar{\Lambda}$ particles, are shown as a function of p_T in pp collisions at $\sqrt{s} = 13$ TeV, for the low multiplicity range $10 \leq N_{\text{trk}}^{\text{offline}} < 20$ (left), and for the high multiplicity $105 \leq N_{\text{trk}}^{\text{offline}} < 150$ (middle). The right plot shows $v_2^{\text{sub}}\{2\}$ results of inclusive charged particles, K_S^0 and $\Lambda/\bar{\Lambda}$ after correcting for back-to-back jet correlations estimated from low-multiplicity data. Statistical and systematic uncertainties are represented, respectively, by bars and shaded boxes. The plots are from Ref. [4].

multiplicity range ($10 \leq N_{\text{trk}}^{\text{offline}} < 20$), which is associated mostly to jet correlations. The middle plot shows v_2 anisotropy coefficient in the high multiplicity range ($105 \leq N_{\text{trk}}^{\text{offline}} < 150$). The residual contribution to long-range correlations from back-to-back jets is estimated and removed by subtracting similar correlations obtained from very low multiplicity pp events. The resulting v_2 is also shown in Fig. 2 (right). No clear mass-ordering for low $N_{\text{trk}}^{\text{offline}}$ ranges is seen in Fig. 2. However, in the high multiplicity $N_{\text{trk}}^{\text{offline}}$ range, a clear mass-ordering is observed, which is indicative of the presence of radial flow. For the subtracted elliptic component $v_2^{\text{sub}}\{2\}$, it can also be seen that for K_S^0 , $v_2^{\text{sub}}\{2\}$ is higher than for $\Lambda/\bar{\Lambda}$ at low p_T , but the order is reversed in the high- p_T range. It can also be seen that the values of $v_2^{\text{sub}}\{2\}$ increase up to $p_T \approx 2 - 3$ GeV/c, and then decrease.

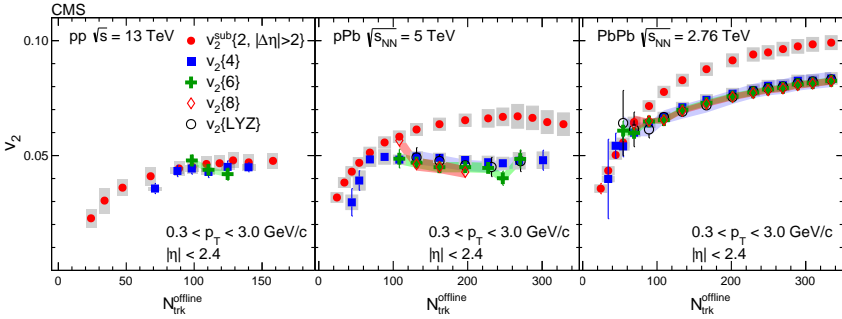


Figure 3. Results from $v_2^{\text{sub}}\{2\}$ and $v_2\{4\}$, $v_2\{6\}$, $v_2\{8\}$ are shown as a function of $N_{\text{trk}}^{\text{offline}}$ for pp collisions in the high multiplicity realm, as well as for pPb and PbPb collisions at the LHC energies, exhibiting a striking similarity in the three systems. Shaded boxes represent systematic uncertainties. Statistical and systematic uncertainties are represented, respectively, by bars and shaded boxes. The plots are from Ref. [4].

The v_2 harmonics are also extracted using the multi-particle cumulant method, in order to search for a possible collective nature of the correlations. The pp data are directly compared to those found

for pPb and PbPb systems over a broad range of similar track multiplicities [4]. The corresponding elliptic flow harmonics v_2 from this study are shown in Fig. 3, which were obtained with the cumulant method in high multiplicity pp collisions at 13 TeV (left), high multiplicity pPb collisions at 7 TeV (middle) and PbPb collisions at 2.76 TeV (right) energies in the nucleon-nucleon center-of-mass. First, the similarity of the results for these very different systems is indeed remarkable, differing mainly for a smaller ratio $v_2\{2\}/v_2\{4\}$ in the case of pp collisions. This smaller ratio perhaps suggests that there are fewer fluctuating sources, leading to less non-flow effects, in the initial conditions of pp collisions as compared to pPb and PbPb. Finally, the most striking result in the pp case, regarding the higher-order cumulants, with $v_2\{2\} \approx v_2\{4\} \approx v_2\{6\}$, clearly shows evidence of collective behavior in pp collisions, as expected from hydrodynamics, which had been already observed earlier in the pPb and PbPb cases. These observations pose an even stronger challenge to theoretical models for explaining the data.

5 Multiparticle azimuthal correlations with symmetric cumulants

In order to further explore the signs suggesting the observation of collectivity in the three systems and refine those measurements, a joint measurement of the anisotropy harmonics (v_n , $n=2-4$) and of event-by-event correlations of different v_n is performed in pp, pPb and PbPb collisions. The v_n results are extracted via long-range ($\Delta\eta > 2$) two-particle correlations as a function of event multiplicity. Event-by-event correlations of v_2 versus v_3 and v_2 versus v_4 are measured using the four-particle Symmetric Cumulant [5] method in all the three systems. Details on the analysis, containing the data samples, trigger and event selections, as well as a description of the techniques employed, and a complete estimate of corresponding systematic uncertainties can be found in can be found in [6].

For extracting the v_n ($n = 2 - 4$) coefficients in the long-range ($\Delta\eta > 2$) two-particle correlations measurements, as already performed in previous CMS papers, first the particle pair distribution is expressed as

$$\frac{dN_{\text{pair}}}{d\Delta\phi} \propto 1 + \sum_n 2V_{n\Delta} \cos(n\Delta\phi), \quad (1)$$

where $V_{n\Delta}$ are the two-particle Fourier coefficients. The single-particle azimuthal anisotropy Fourier coefficients v_n can then be extracted as $v_n = \sqrt{V_{n\Delta}}$, assuming that factorization applies [12].

The SC technique was first introduced by the ALICE collaboration[5] in LHC measurements and is based on a 4-particle correlation calculations with cumulants. The difference between the standard cumulant calculation and the SC is that the first is used to compute diagonal v_n terms and the latter is used for measuring correlations between different coefficient orders. Therefore, to study the correlation between a harmonic n and m , one can build 2- and 4-particle correlator with: $\langle\langle 2 \rangle\rangle_n = \langle\langle e^{i(n\phi_1 - m\phi_2)} \rangle\rangle \sim \langle v_n^2 \rangle$ and $\langle\langle 4 \rangle\rangle_{n,m} = \langle\langle e^{i(n\phi_1 + m\phi_2 - n\phi_3 - m\phi_4)} \rangle\rangle \sim \langle v_n^2 v_m^2 \rangle$. The measured observable of the Scalar Product method, $\text{SC}(n, m)$, is then defined as

$$\text{SC}(n, m) = \langle\langle 4 \rangle\rangle_{n,m} - \langle\langle 2 \rangle\rangle_n \cdot \langle\langle 2 \rangle\rangle_m = \langle v_n^2 v_m^2 \rangle - \langle v_n^2 \rangle \langle v_m^2 \rangle. \quad (2)$$

Details of the procedure corresponding to the two methods ca be found in [6].

The measurements of v_2 , v_3 , and v_4 coefficients for $0.3 < p_T < 3$ GeV/c from long-range two-particle correlations are shown in Fig. 4, as a function of multiplicity in 13 TeV pp, 5.02 and 8.16 TeV pPb, and 5.02 TeV PbPb collisions. The contribution to v_n coefficients from back-to-back jet correlations are corrected by subtracting correlations from very low-multiplicity events (v_n^{sub}), as done in Refs. [4, 13]. The v_n results before subtraction are also shown as lines in this figure. The effect of the low-multiplicity subtraction for $N_{\text{trk}}^{\text{offline}} > 200$ is very small in pPb and PbPb collisions. At

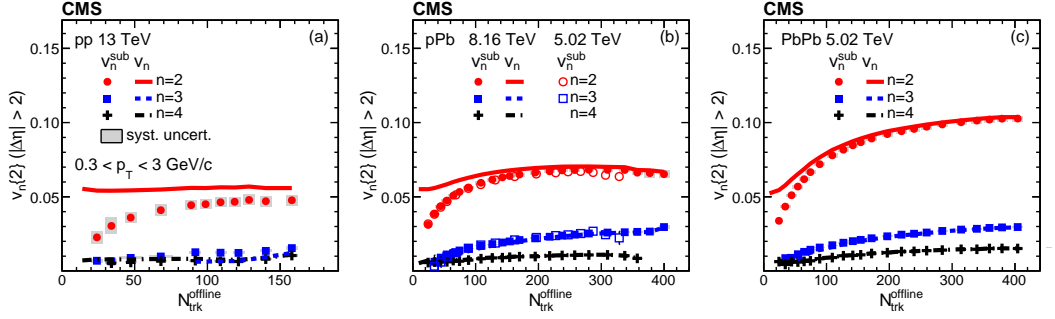


Figure 4. The v_2 , v_3 [4], and v_4 coefficients from long-range two-particle correlations are shown as a function of $N_{\text{trk}}^{\text{offline}}$ in 13 TeV pp (a), 5.02 TeV pPb (b), and 8.16 TeV pPb (b), and 5.02 TeV PbPb collisions (c). The results corrected by low-multiplicity subtraction are denoted as v_n^{sub} . The lines show the v_n results before subtraction of low-multiplicity correlations. The gray boxes represent systematic uncertainties. The plots are from Ref. [6].

low multiplicities, however, this correction is significant, in particular for pp collisions where dijet correlations are expected to be the main source of correlations. Due to the higher collision energy and integrated luminosity, the new 8.16 TeV pPb results allowed for extending the measurements of the v_n coefficients to higher multiplicities as compared to the 5.02 TeV pPb data. Still from Fig. 4, it can be seen that the v_2 coefficient increases with $N_{\text{trk}}^{\text{offline}}$, saturating for values of this variable above 200. It can also be seen that v_4 has finite values in all three systems, being about 50% smaller than the v_3 coefficients for $N_{\text{trk}}^{\text{offline}} > 100$, mainly visible in the pPb and PbPb results.

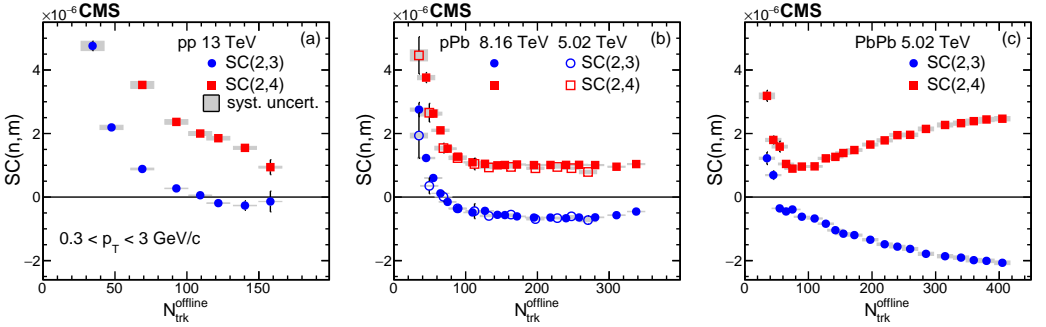


Figure 5. The SCs for the second and third coefficient (red points) and the second and fourth coefficient (blue points) as a function of $N_{\text{trk}}^{\text{offline}}$ in 13 TeV pp (a), 5.02 TeV and 8.16 TeV pPb (b), and 5.02 TeV PbPb collisions (c). The gray boxes represent systematic uncertainties. The plots are from Ref. [6].

Results from symmetric cumulants allow to further study the correlations of different v_n coefficients. The measurements of SC(2,3) and SC(2,4), for $0.3 < p_T < 3$ GeV/c from four-particle correlations, are shown in Fig. 5, as a function of multiplicity in 13 TeV pp, 5.02 and 8.16 TeV pPb, and 5.02 TeV PbPb. From this figure, it can be seen that both SC(2,3) and SC(2,4) decrease as $N_{\text{trk}}^{\text{offline}}$

increases in pp collisions. The $SC(2, 4)$ values always remain positive, while an indication of a transition to negative values for $SC(2, 3)$ can be envisaged for $N_{\text{trk}}^{\text{offline}} > 110$, although the measurement is not precise enough to allow for a firm conclusion. For pPb and PbPb data at sufficiently high multiplicities (e.g., $N_{\text{trk}}^{\text{offline}} > 60$), clear negative values of $SC(2, 3)$ are observed, while $SC(2, 4)$ values are positive in all the multiplicity range. Besides, it can be seen that the PbPb data are consistent with the results reported at $\sqrt{s_{NN}} = 2.76$ TeV [5]. In lower multiplicity ranges ($N_{\text{trk}}^{\text{offline}} < 100$) for all three systems, both $SC(2, 3)$ and $SC(2, 4)$ have positive values, which increase as $N_{\text{trk}}^{\text{offline}}$ decreases. Nevertheless, in the low multiplicity region, short-range few-body correlations, such as in jets, are likely to have a dominant contribution, which needs to be properly taken into account. Besides, the jet contribution at low $N_{\text{trk}}^{\text{offline}}$ might be different in pp, pPb and PbPb, and perhaps could account for the slightly different behaviors of the SCs observed in the data in this multiplicity range.

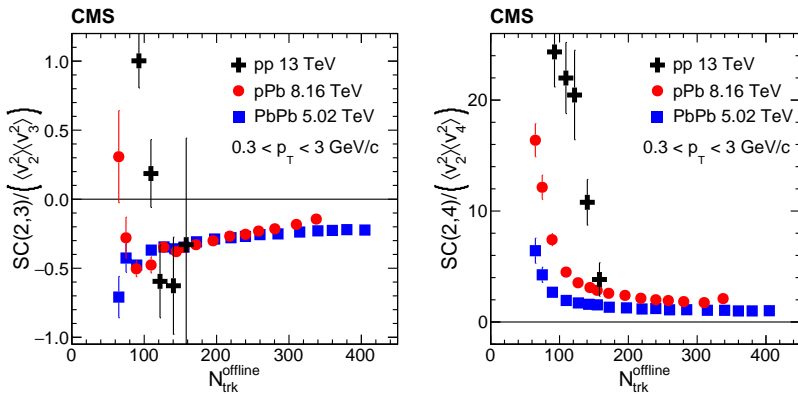


Figure 6. The SCs for the second and third coefficients (left) and the second and fourth coefficients (right) normalized by $\langle (v_2^{\text{sub}})^2 \rangle \langle (v_3^{\text{sub}})^2 \rangle$ and $\langle (v_2^{\text{sub}})^2 \rangle \langle (v_4^{\text{sub}})^2 \rangle$ from two-particle correlations. The track p_T range is $0.3 < p_T < 3$ GeV/c and the results are shown as a function of $N_{\text{trk}}^{\text{offline}}$ in 13TeV pp, 8.16TeV pPb, and 5.02 TeV PbPb collisions. The plots are from Ref. [6].

In Fig. 5, the absolute magnitudes of $SC(2, 3)$ and $SC(2, 4)$ are seen to be larger in PbPb as compared to pPb systems at high multiplicities. However, this may be related to the different magnitude of v_n coefficients as seen in Fig. 4. Therefore, to investigate intrinsic correlations between v_n coefficients and compare with different collision systems in a more quantitative way, $SC(2, 3)$ and $SC(2, 4)$ are normalized by $\langle (v_2^{\text{sub}})^2 \rangle \langle (v_3^{\text{sub}})^2 \rangle$ and $\langle (v_2^{\text{sub}})^2 \rangle \langle (v_4^{\text{sub}})^2 \rangle$, respectively, based on the v_n values from two-particle correlations in Fig. 4. One must note that the two-particle correlation v_n with a rapidity gap is used for the normalization, therefore, the results could be affected by the event-plane decorrelation as measured in [15] within a few percent. Nevertheless, all systems would be affected consistently, so that the conclusions from the results would remain unchanged. The resulting normalized SCs in all three colliding systems are shown in Fig. 6. The normalized $SC(2, 3)$ values are found to be very similar between pPb and PbPb systems at high multiplicities. Taken together with the v_n results in Fig. 4, these measurements strongly suggest a unified origin to explain the collective behavior observed in large and small hadronic collisions. It is interesting to note that this common behavior may even apply to pp collisions for $N_{\text{trk}}^{\text{offline}} > 120$, where $SC(2, 3)$ tends to converge to a unified value for all three systems, even though the statistical uncertainties are still too large to draw a firm conclusion. The $SC(2, 4)$, on the other hand, shows a clear dependence on the system size with a larger value

for smaller systems. Complementary, the observed difference between SC(2,4) values in pPb and PbPb collisions, however, may point to a different contribution of initial-state fluctuations or transport properties of the medium such as the shear viscosity to entropy ratio [14].

6 Summary and conclusions

Several measurements with data collected with the CMS experiment and related to azimuthal anisotropy correlations were reported here. The first, with charged particles produced in PbPb collisions at $\sqrt{s_{NN}} = 5.02$ TeV, in which v_2 and v_3 coefficients were determined for different collision centralities, extending over the widest transverse momentum range studied to date ($1 < p_T < 100$ GeV/c). Positive v_2 values were found up to $p_T \approx 70$ GeV/c, while for v_3 , the values are consistent with zero for $p_T > 20$ GeV/c. For $p_T < 3$ GeV/c, it is observed that $v_2\{\text{SP}\} > v_2\{4\} \approx v_2\{6\} \approx v_2\{8\}$, which is consistent with a collective behavior arising from the hydrodynamic expansion of a quark-gluon plasma and such similarity of $v_2\{4\}$, $v_2\{6\}$, and $v_2\{8\}$ at high p_T suggests that v_2 originates from the path-length dependence of parton energy loss associated with an asymmetric initial collision geometry.

Data collected in pp collisions at $\sqrt{s} = 13$ TeV have been used to measure two- and multi-particle azimuthal correlations with unidentified charged particles (h^\pm), as well as reconstructed K_s^0 and Λ particles, exploring the correlation data over a broad particle multiplicity range. The v_2 and v_3 Fourier coefficients are extracted from long-range two-particle correlations, from which contributions from back-to-back jet correlations, estimated using low-multiplicity data, are subtracted. In the higher-multiplicity region, a particle species dependence of v_2 is observed with and without correcting for jet correlations, a similar behavior to what had been observed for identified particles produced in pPb and AA collisions at RHIC and the LHC. Even more striking is the observation that the v_2 values obtained with 2-, 4-, and 6-particle correlations at $\sqrt{s} = 13$ TeV, are found to be comparable within uncertainties, providing strong evidence in support of a collective origin for the observed long-range correlations in high-multiplicity pp collisions.

The v_2 , v_3 , and v_4 Fourier coefficients are extracted from long-range two-particle correlations for 8.16 TeV pPb collisions and compared to those in 13 TeV pp, 5.02 TeV pPb and 5.02 TeV PbPb results. Using a four-particle cumulant technique, correlations between different coefficients are obtained. A negative (positive) correlation is observed between v_2 and v_3 (v_4) in pPb collisions, similarly to what is observed in PbPb systems. Normalized correlation coefficients for v_2 and v_3 are found to be quantitatively similar between pPb and PbPb, whereas the results for v_2 and v_4 are larger in pPb than in PbPb. The corresponding result in pp collisions shows a similar trend at high multiplicity as in pPb and PbPb, however, the statistical uncertainties do not allow for a firm conclusion.

The set of measurements discussed above shows results which provide evidence of collectivity in pp, pPb and PbPb systems alike, suggesting that the observed behavior in data may have a similar origin. This represent a considerable challenge to theoretical models, imposing significant constraints in their tentative to explain the experimental findings.

References

- [1] M. Gyulassy and L. McLerran, *New forms of QCD matter discovered at RHIC*, Nucl. Phys. **A750** (2005) 30.
- [2] CMS Collaboration, *Observation of Long-Range Near-Side Angular Correlations in Proton-Proton Collisions at the LHC*, JHEP **09** (2010) 091, doi:10.1007/JHEP09(2010)091, arXiv:1009.4122.

- [3] CMS Collaboration, *High- p_T track v_n harmonics in PbPb collisions at 5.02 TeV*, submitted to Phys. Lett. **B**, arXiv:1702.00630 [hep-ex].
- [4] CMS Collaboration, *Evidence for collectivity in pp collisions at the LHC*, Phys. Lett. **B** 765 (2017) 193, arXiv:1606.06198.
- [5] ALICE Collaboration, *Correlated event-by-event fluctuations of flow harmonics in PbPb collisions at $\sqrt{s_{NN}} = 2.76$ TeV*, Phys. Rev. Lett. **117** (2016) 182301, arXiv:1604.07663.
- [6] CMS Collaboration, *Observation of correlated azimuthal anisotropy Fourier harmonics in pp and pPb collisions at the LHC*, submitted to Phys. Rev. Lett., arXiv:1709.09189 [hep-ex].
- [7] CMS Collaboration, *The CMS experiment at the CERN LHC*, JINST **0803** (2008) S08004.
- [8] J. Noronha-Hostler, B. Betz, J. Noronha, and M. Gyulassy, *Event-by-Event Hydrodynamics + Jet Energy Loss: A Solution to the RAA \otimes v_2 Puzzle*, Phys. Rev. Lett. **116** (2016) 252301, doi:10.1103/PhysRevLett.116.252301, arXiv:1602.03788.
- [9] J. Xu, J. Liao, and M. Gyulassy, *Bridging soft-hard transport properties of Quark-Gluon Plasmas with CUJET3.0*, JHEP **02** (2016) 169, doi:10.1007/JHEP02(2016)169, arXiv:1508.00552.
- [10] M. Luzum and J.-Y. Ollitrault, *Eliminating experimental bias in anisotropic-flow measurements of high-energy nuclear collision*, Phys. Rev. **C87** (2013), n. 4, 044907, doi:10.1103/PhysRevC.87.044907, arXiv:1209.2323.
- [11] A. Bilandzic et al., *Generic framework for anisotropic flow analyses with multiparticle azimuthal correlations*, Phys. Rev. **C89** (2014), no. 6, 064904, doi:10.1103/PhysRevC.89.064904, arXiv:1312.3572.
- [12] S. Voloshin and Y. Zhang, *Flow study in relativistic nuclear collisions by Fourier expansion of azimuthal particle distributions*, Z. Phys. **C 70** (1996) 665, doi:10.1007/s002880050141, arXiv:hep-ph/9407282.
- [13] CMS Collaboration, *Multiplicity and transverse momentum dependence of two- and four-particle correlations in pPb and PbPb collisions*, Phys. Lett. **B 724** (2013) 213, doi:10.1016/j.physletb.2013.06.028, arXiv:1305.0609.
- [14] K. Welsh, J. Singer, and U. W. Heinz, *Initial state fluctuations in collisions between light and heavy ions*, Phys. Rev. **C 94** (2016) 024919, doi:10.1103/PhysRevC.94.024919, arXiv:1605.09418.
- [15] CMS Collaboration, *Evidence for transverse momentum and pseudorapidity dependent event plane fluctuations in PbPb and pPb collisions*, Phys. Rev. **C 92** (2015) 034911, doi:10.1103/PhysRevC.92.034911, arXiv:1503.01692.